Ultrawide band gaps in beams with double-leaf acoustic black hole indentations

Liling Tang, and Li Cheng

Ultrawide band gaps in beams with double-leaf acoustic black hole indentations

Liling Tang and Li Cheng[a)]

Department of Mechanical Engineering, The Hong Kong Polytechnic University, Hung Hom, Kowloon, Hong Kong 999077, China

Band gaps in conventional phononic crystals (PCs) are attractive for applications such as vibration control, wave manipulation, and sound absorption. Their practical implementations, however, are hampered by several factors, among which the large number of cells required and their impractically large size to ensure the stopbands at reasonably low frequencies are on the top of the list. This paper reports a type of beam carved inside with two double-leaf acoustic black hole indentations. By incorporating the local resonance effect and the Bragg scattering effect generated by a strengthening stud connecting the two branches of the indentations, ultrawide band gaps are achieved. Increasing the length of the stud or reducing the residual thickness of the indentation allows the tuning of the band gaps to significantly enlarge the band gaps, which can exceed 90% of the entire frequency range of interest. Experimental results show that with only three cells, the proposed beam allows considerable vibration energy attenuation within an ultra-broad frequency range including the low frequency range, which conventional PCs can hardly reach. Meanwhile, the proposed configuration also enhances the structural integrity, thus pointing at promising applications in vibration control and a high performance wave filter design. © *2017 Acoustical Society of America.* https://doi.org/10.1121/1.5009582

I. INTRODUCTION

Phononic crystals (PCs)[1] are artificial media consisting of periodic materials or components with the ability to achieve unusual wave propagation characteristics, such as waves filtering,[2,3] negative refraction,[4,5] band gaps,[6–8] etc. Owing to the Bragg scattering[9,10] or local resonance[11–13] mechanisms, band gaps are shown to exist in PCs, thus showing great potentials for applications such as vibration control, wave manipulation and sound absorption, etc. However, problems exist in both types of band gaps, which somehow hamper the practical applications of the conventional PCs. Bragg scattering leads to broad band gaps only at sub-wavelength scale when the lattice constant exceeds the wavelength. Therefore, for low frequency and long wavelength wave attenuation, the unit cell may become prohibitively large. Meanwhile, a large number of cells are usually required to obtain the desired band gaps. These limitations can, to a certain extent, be overcome by the locally resonant band gaps through attaching local resonators to the host structures.[14–16] The local resonant gaps, however, are usually narrow. The combined use of Bragg scattering and local resonant effects can, in principle, result in wider and lower-frequency band gaps. The improvement obtained, however, is somehow limited to a certain frequency range in the cases reported in the open literature.[17,18] Although a topological optimization is also attempted to achieve broader band gaps, the optimized unit cells usually have complex geometry which is difficult to fabricate.[19–22] In a different prospective, most PCs are usually tied with the inherent structural

weakness due to the multiple structural interfaces, which are needed to create structural impedance changes. Therefore, the search for PCs with broad band gaps in both low and mid-high frequency range while ensuring acceptable structural properties without attaching additional elements and multiple interfaces becomes important.

The advent of the acoustics black holes (ABH) phenomenon offers a new perspective to resolve the aforementioned problem. The ABH effect allows manipulating flexural wave propagation inside a thin-walled structure, with its thickness tailored according to a power-law variation, typically $h(x) = \varepsilon x^m (m \geq 2)$ in one dimensional cases.[23,24] In an idealized ABH structure, the phase and group velocities of the flexural waves gradually reduce to zero at the tip of the taper, thus annulling wave reflection. When this happens, the tapered ABH becomes an ideal energy absorber because of the high energy concentration and trapping. Despite the inevitable truncated thickness of the structures in practice (also referred to as residual thickness hereafter), considerable energy focalization of the ABH effect can still be observed.[25,26] The ABH-specific energy focalization in a plate with embedded conventional ABH cells is shown to generate unique dispersion properties.[27] Applications of the ABH-like profiles in various meta-surfaces were also attempted in the realization of anomalous refraction, focal lenses and phase masks.[28] However, due to the complex wave travel paths in a 2D system, whether absolute band gaps exist still remains unknown. Owing to the relatively simple wave travel path in 1D structures, our previous work first shows the locally resonant band gaps in an Euler-Bernoulli beam by taking advantages of the energy focalization of the ABH effect.[29] The observed band gaps, albeit

a)Electronic mail: li.cheng@polyu.edu.hk

much broader than conventional locally resonant bandgaps, are limited to relatively low frequency range. Besides, similar to Ref. 27, the structure still inherits the existing structural weakness problems due to the extremely thin residual thickness of the conventional ABH cells. Double-layered ABH indentations have first been incorporated into composite panels for structural damping enhancement.[30] Such a design has been shown to provide better static and dynamic properties compared with conventional single-layered ABH structures.[31] However, structures with periodic double-layered ABH indentations and possible induced accumulated ABH effect have not been investigated.

In the present work, we propose a new type of beam structures, by capitalizing on the unique energy focalization feature of the ABH effect and by exploring the dual benefit of the local resonance and Bragg scattering effect. In the proposed design, the ABH indentations with a power-law thickness profile are carved inside of a uniform unit cell to create locally resonant band gaps while ensuring good structural stiffness/strength. Meanwhile, to produce the coupling effect of Bragg scattering and local resonances, a crosspiece connecting the two branches of the indentations (referred to as a strengthening stud) is added in the hollowed ABH area. This allows the generation of ultrawide band gaps nearly over the entire frequency range without complex geometry and add-on attachment from outside of the structure. The band structures and their generation mechanism of the proposed beams (with and without studs) are first analyzed and compared in Sec. II. Key parameters, i.e., the stud length and the residual thickness of ABHs, are investigated in views of possible tuning of the band gaps. Experiments on finite beams, using only three ABH cells, are then carried out in Sec. III to validate the numerically observed band gaps. Finally, the conclusions are drawn.

II. BAND STRUCTURES OF PHONONIC BEAMS

The proposed beam consists of a uniform beam lattice with its inside being carved by a double-leaf ABH tapered profile, whose thickness variation is described as $h(x) = \varepsilon x^m + h_0$.[32] The unit cell design and geometrical parameters are shown in Fig. 1. The design ensures the structural integrity on the lattice surface and relatively high
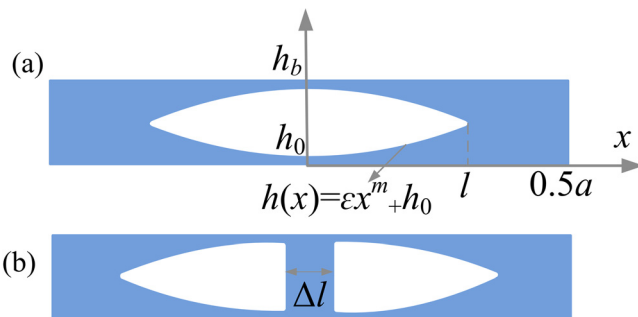
structural stiffness and strength, empowering the beams with reasonable transverse load-bearing capability. In the analyses, the unit cell length $a = 0.12$ m and the beam thickness $h_b = 0.0064$ m. Each branch takes the form of $h(x) = 3x^2 + 0.0005$ with a residual thickness $h_0 = 0.0005$ m and the length l is set to be 0.03 m. The unit cell is made of steel with a mass density of 7800 kg/m^3, Young's modulus of 210 Gpa, and Poisson's ratio of 0.3. The band structures are calculated using finite element analysis software COMSOL MULTIPHYSICS v5.2. Because of the non-uniform profile, 2D unit cells are modeled through sufficiently dense mesh with triangular elements in solid mechanics module. The Floquet periodic boundary condition is imposed at the edges of the unit cell and a parametric sweep is applied over the reduced wave vector k. Note that only flexural waves are considered.

Beams without the strengthening stud ($\Delta l = 0$) are first considered with their band structures depicted in circles in Fig. 2. A non-dimensional frequency, $f_R = fa/c$, is included in the right vertical coordinate as a reference with c being the flexural wave velocity in the uniform part (Note other frequency terms used in the following discussion are also normalized with c/a.) The first two broad band gaps are obtained with the normalized bandwidth $\Delta f/f_c = 86.3\%$ and 110%, respectively, where Δf is the bandwidth and f_c is the center frequency of the gap. These two band gaps are rather flat, which means that the slope of the dispersion curves is almost zero. In this case, the group velocity of the wave also approaches zero, indicating that the waves stop propagating and are confined to a region. Representative mode shapes are depicted in Fig. 3. For the mode indicated by A, the vibration mainly concentrates on the ABH indentation with negligible motion in the uniform part of the cell. This can be attributed to the unique energy focalization feature of the ABH phenomenon. The gradual thickness changes in the ABH

FIG. 1. (Color online) Unit cells of the proposed phononic beams with the same lattice constant a and beam thickness h_b: (a) carved inside according to $h(x) = \varepsilon x^m + h_0$ with a length l and a residual thickness h_0; (b) the same symmetrical tapered profiles are embedded and connected by a strengthening stud of length Δl.
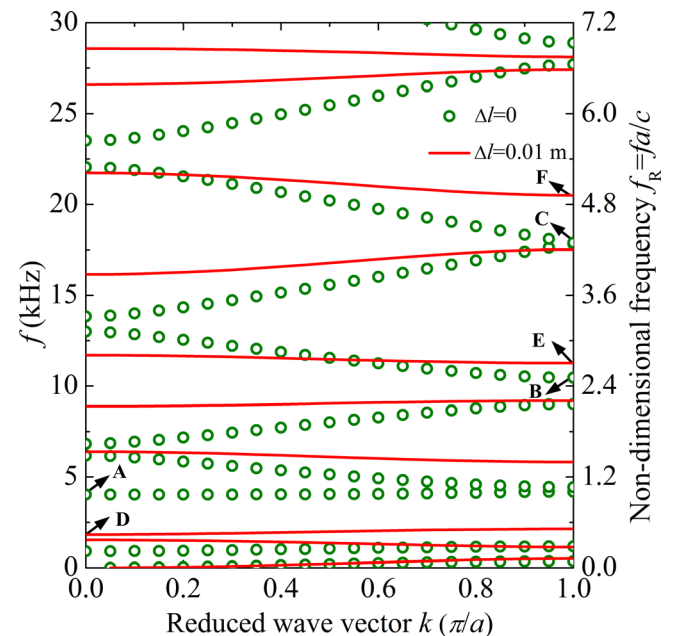

FIG. 2. (Color online) Band structures for the phononic beams with ABH cells. Circles: without strengthening studs ($\Delta l = 0$); lines: with studs ($\Delta l = 0.01$ m).

J. Acoust. Soc. Am. **142** (5), November 2017
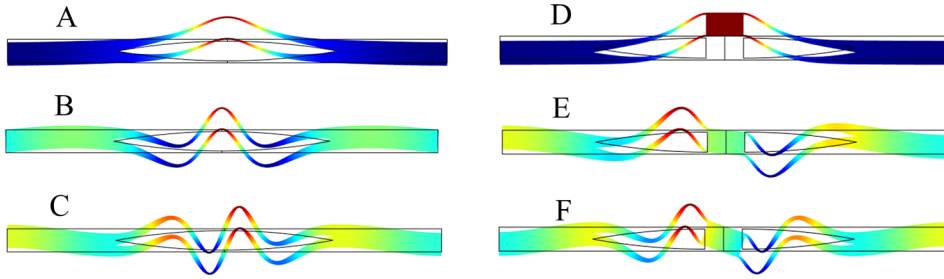
Liling Tang and Li Cheng   2803

FIG. 3. (Color online) Displacement field of typical modes marked by A-F in the band structure curves in Fig. 2.

indentation produce strong energy focalization as a result of the gradual slowing-down of the incoming wave speed toward the indentation center. This is manifested by a compression of the bending waves with a reducing wavelength and increasing vibration amplitude. As a result, this highly dynamic region generates energetic locally resonant modes which are responsible for the band gaps in the low frequency region, similar to the case of conventional ABH configurations.[29] Moreover, the present ABH indentation acts as continuous local resonators with multiple degrees of freedom, thus generating multiple locally resonant and broad bandgaps, different from the conventional narrow local band gaps induced by single-degree-of-freedom spring mass resonators. However, the local resonance effect is gradually impaired when the uniform part is activated as the frequency increases, exemplified by modes B and C shown in Fig. 3. As a result, the band gaps become narrower at higher frequencies, typically with the normalized bandwidth below 10% (Fig. 2).

To further enlarge the band gaps at the mid-to-high frequency region, a strengthening stud of length $\Delta l = 0.01$ m is added as sketched in Fig. 1(b). The corresponding band structures are also given in Fig. 2 in solid lines for comparison with the case without the stud ($\Delta l = 0$). As can be seen, while retaining the band gaps at low frequencies, nearly all the mid-to-high frequency ranges (typically when $f_R > 1$) are covered by wide and flat band gaps, with normalized bandwidth ranging from 15% to 32%. The displacement field of the selected modes in Fig. 3 is similar to the case without the studs; namely, ABH-induced local resonances dominate the low frequency region (see mode D) but are weakened at mid-to-high frequencies (see modes E and F). The difference is that the strengthening stud causes a large impedance mismatch with the thin ABH indentation tip, which ensures the generation of the Bragg scattering at mid-to-high frequencies. Owing to the strong energy concentration within the indentation area, high intensity waves are reflected with an accelerating velocity (due to the increase in the structural thickness this time) when reaching the studs. The combination of local resonance and Bragg scattering effect produces these broad band gaps.

In views of performance tuning or eventually optimization, we investigate the influence of the length Δl on the band structures. Figure 4 plots the normalized band gaps for different normalized stud lengths $\Delta l/a$. It can be seen that the band gaps in the mid-to-high frequency range are drastically enlarged with even an extremely short stud length ($\Delta l/a = 1/60$, for example). Further increasing $\Delta l/a$ would allow the tuning of the band gaps, in both their central

frequency and the associated bandwidth. It can be seen that when $\Delta l/a = 1/4$, a significant portion of the frequency range is filled with band gaps. To quantify the frequency coverage of the band gaps, the ratio between the sum of the bandwidth of all band gaps, $\Sigma \Delta f$, and the entire normalized frequency range, f_s, is calculated, with results compared in Fig. 5 for different normalized stud lengths. It confirms again that the addition of the stud, albeit very short, brings about immediate benefit to the enlargement of the band gaps. Further increasing the stud length, although still beneficial, only offers gradual improvement.

It is worth noting that enhancing energy focalization of the ABH effect by increasing the taper power index m without violating the smoothness criterion[33] or reducing the residual thickness h_0 is beneficial to prompt the ABH indentation as ideal local resonators, thus generating broader low frequency band gaps.[29] Meanwhile, the reduced residual thickness h_0 would lead to larger impedance mismatch with the strengthening stud. Consequently, Bragg scattering can further be strengthened to create even broader band gaps at the mid-to-high frequencies. As an example, Fig. 6 shows
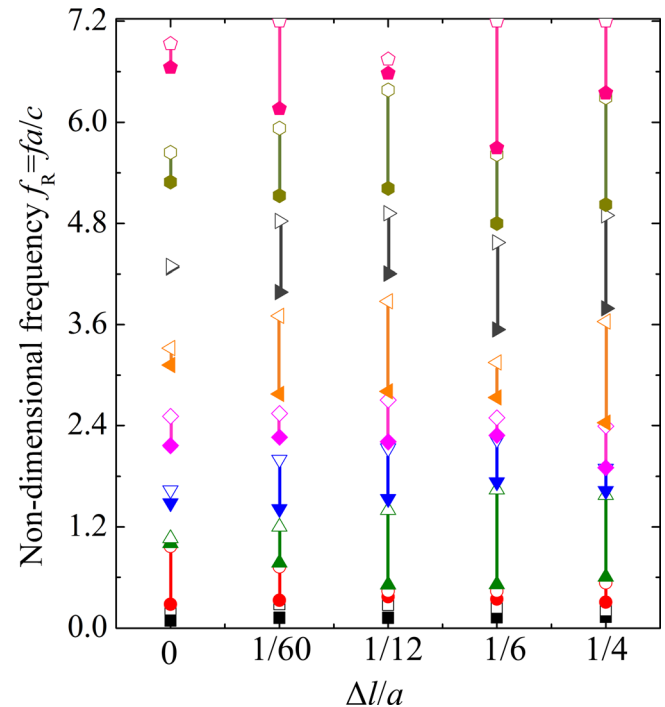

FIG. 4. (Color online) Band gaps vs normalized stud length $\Delta l/a$. Solid and open symbols denote the lower and upper boundaries of the band gaps, respectively; lines between symbols represent the bandwidth of different band gaps (identified using different colors and symbols).
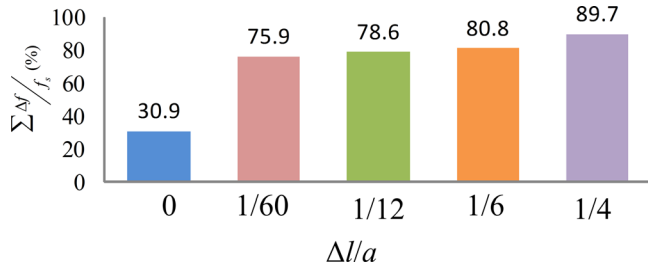
Liling Tang and Li Cheng

FIG. 5. (Color online) Ratio between the sum of bandwidths of band gaps and the entire frequency range $\Sigma \Delta f / f_s$, where f_s equals to 7.2 in the present study.

the band structures of a phononic beam with the same geometrical parameters as those used in Fig. 2, but with the residual thickness of the ABH indentation being reduced by half, i.e., $h_0 = 0.00025$ m. As can be seen, flat and broad band gaps cover nearly the entire frequency range, owing to the enhanced effect from both local resonances and Bragg scattering. The bandwidth percentage $\Sigma \Delta f / f_s$ increases up to 92%, as compared to 78.6% when $h_0 = 0.0005$ m.

III. EXPERIMENTAL VALIDATIONS

Note that above analyses concern beams of infinite length with periodic ABH lattice, which can be referred to as phononic beams. In practice, however, it is relevant to investigate practical ways to achieve the desired band gap properties in a beam of finite length with only a small number of ABH cells. To this end, experiments were carried out and compared to numerical results using two fabricated finite beams consisting of three cells with the same geometrical and material parameters used in Fig. 2. A uniform beam with the same length was also tested as a reference, as shown in Fig. 7(a). In all cases, the width of the three beams remains the same (0.01 m). Flexural vibration responses of the beams
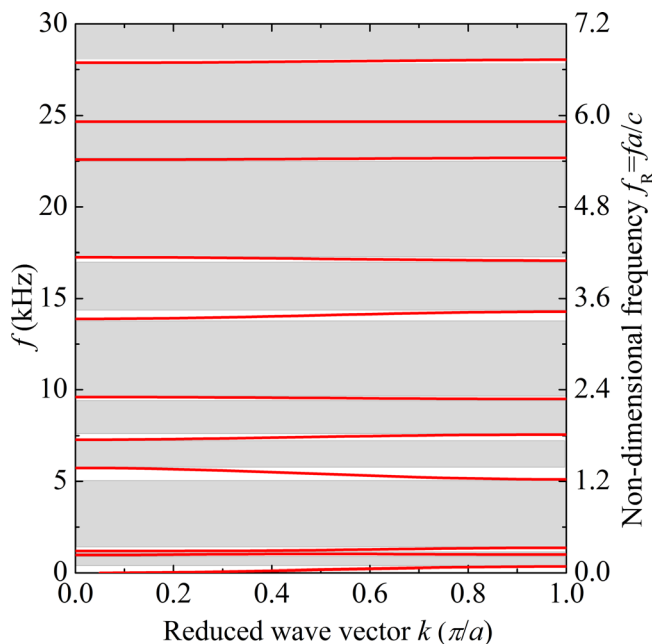

FIG. 6. (Color online) Band structures for the phononic beams with $h_0 = 0.00025$ m. All other geometrical parameters are the same as those used in Fig. 2 ($\Delta l = 0.01$ m). The grey areas denote band gaps.
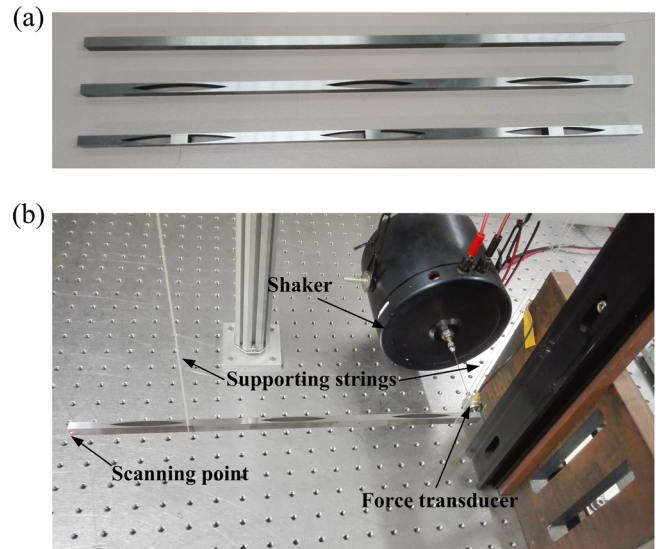

FIG. 7. (Color online) (a) a uniform beam and two beams with the same material and geometrical parameters as those used in Fig. 2. (b) Experiment setup.

when subjected to a unit point excitation force were analysed. The experiment setup is shown in Fig. 7(b). The beams were supported with two thin strings to mimic free boundaries. A periodic chirp signal from 0 to 20 kHz was applied at one end of the beams through an electromagnetic shaker, with the excitation force measured by a force transducer (B&K 8200) and amplified by a charge amplifier (B&K 2635). A Polytec scanning laser vibrometer was used to scan the whole beam for the response measurement.

Figure 8 shows the comparison between the displacement transmission, defined as $20 \log w_{out} / w_{in}$ (w_{out} and w_{in} are, respectively, the output and input of displacement), from experiments and numerical simulations. For easy comparison, the case of the uniform beam is also included in both Figs. 8(a) and 8(b). Without particular treatment, the uniform beam exhibits no particular wave filtering ability. From Fig. 8(a), we can see several obvious attenuation gaps below 5 kHz, which are in good agreement with the observed band gaps in Fig. 2. The experimental results agree reasonably well with the numerical results with only a few additional peaks in the attenuation gaps. This can be attributed to the torsional waves, induced by the slight deviation of excitation force from the central axis of the beam. The torsional waves emerge when flexural waves became significantly weak within the band gaps. For the same reason, signals became noisier within the attenuation gaps. Without the strengthening studs, the attenuation gaps barely exist apart from the low frequency region, in agreement with the numerical analyses. When three strengthening studs with a length $\Delta l = 0.01$ m were added, Fig. 8(b) shows several attenuation gaps, which agree with the numerically predicted band gaps shown in Fig. 2. These attenuation bands cover a very large portion of the frequency range, generating transmission attenuation up to nearly 60 dB. Once again, experimental results agree well with numerical ones in terms of both location and width of the attenuation bands. Differences in the deep trough areas are due to the same reasons as stated above. It is relevant to note that, as a side

J. Acoust. Soc. Am. **142** (5), November 2017
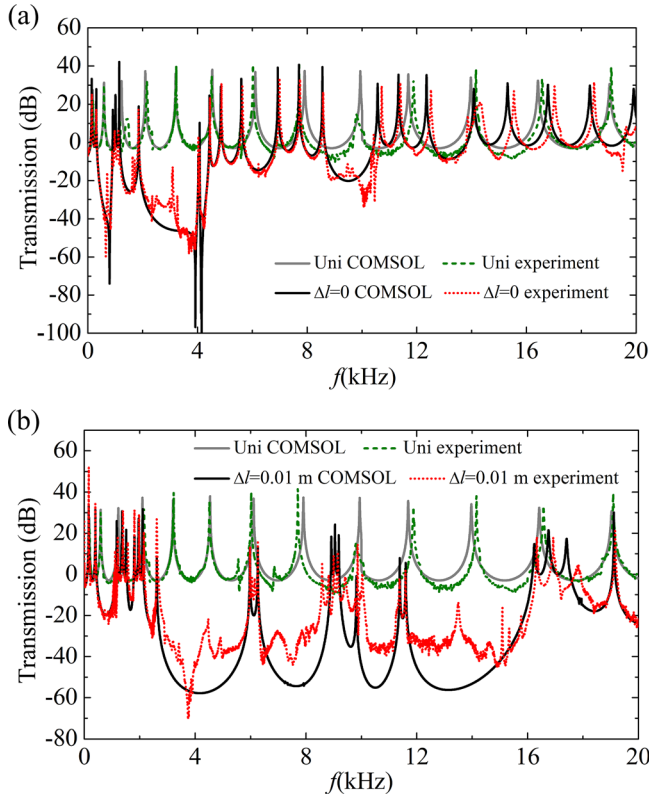
Liling Tang and Li Cheng   2805

FIG. 8. (Color online) Displacement transmission comparison between the numerical results (grey and dark solid lines) and experiment results (green dashed and red dotted lines): (a) the beam with $\Delta l = 0$ and (b) the beam with $\Delta l = 0.01$m; the uniform beam included in both case as a reference.

FIG. 9. (Color online) Displacement distribution of (a) the beam with $\Delta l = 0$ for $f = 3506$ Hz and (b) the beam with $\Delta l = 0.01$ m for $f = 4280$ Hz. Different highlighted-color areas present different cells with cell 1 nearest to the excitation end.

benefit of the ABH effect, the levels of the transmission peaks are also reduced compared with the uniform beam at mid-to-high frequencies.

The above comparisons show that, with only three cells, the proposed beams exhibit remarkable wave attenuation ability. The displacement distribution at two chosen frequencies within the attenuation bands are plotted in Fig. 9 to further reveal the vibration attenuation effect. For both beams with ABH indentations, the measured displacement matches well with the numerically calculated one. It can be seen that the vibration is reduced prominently as the wave propagates through cells in both cases. With the strengthening studs, the vibration reduction is more significant compared with its counterpart without studs, in agreement with numerical analyses.

IV. CONCLUSIONS

In the present work, we propose a new type of beam with embedded double-leaf ABH indentations. Using an infinite beam lattice, the band structures and their generation mechanism are analyzed and compared through finite element analyses. Key parameters, i.e., the length of the strengthening studs and the residual thickness of the ABH indentation are investigated to tune the band gaps in terms of their bandwidth and distribution. Experiments are conducted to confirm and validate the numerically predicted phenomena using beams of finite length containing only a small number of ABH cells. The main conclusions are summarized as follows.
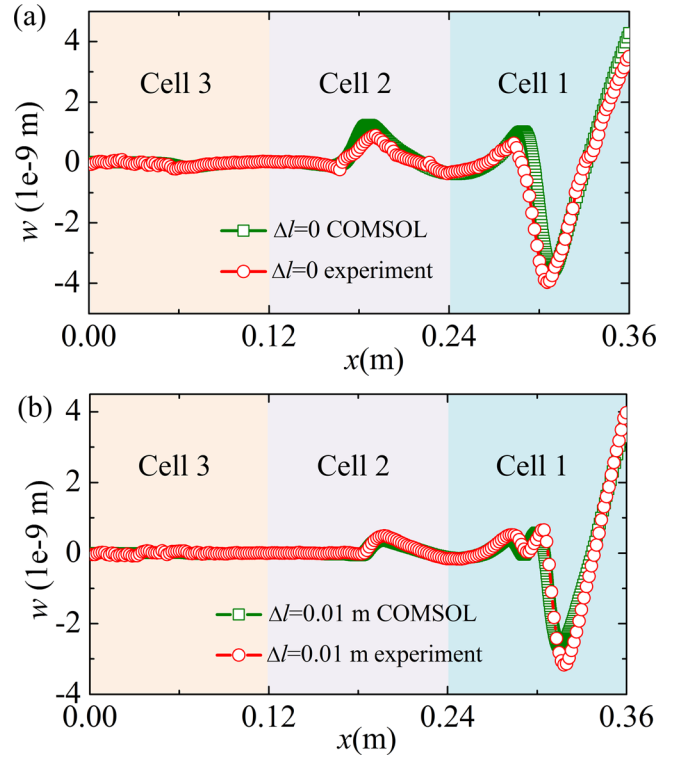
The proposed phononic beams with double-leaf tapered profiles carved inside a uniform unit cell are shown to exhibit remarkable band gap properties. The unique energy focalization feature of the ABH effect offers the dual benefit: effective and energetic local resonant modes at relatively low frequencies and intensive wave interferences to generate Bragg scattering when the strengthening studs are added. As a result, the two effects are combined to produce ultrawide band gaps. The impedance mismatch between the stud and the thin ABH indentation, responsible for the generation of the Bragg scattering, can be tuned by changing various parameters related to the ABH indentations and the strengthening studs. Increasing the length of the stud or reducing the residual thickness of ABH indentation allows a significant increase in the gap bandwidth, which can cover nearly 90% of the entire frequency range of interest with realistic geometric and material parameters considered in this paper. The numerically predicted phenomena are confirmed by experiments, which further show that, with only three cells, the proposed beams warrant considerable vibration attenuation.

As to the structure itself, the proposed beams, through embedding tapered profiles inside the uniform beams, ensure the structural integrity on the surface while improving the inherent structural stiffness/strength weakness of conventional ABH structures in terms of load-bearing capability. Compared with most conventional PCs using add-on resonators or optimized complex geometries, the proposed structures are self-also self-contained and easier to fabricate, offering great potentials for various applications.

Liling Tang and Li Cheng

[1]M. H. Lu, L. Feng, and Y. F. Chen, "Phononic crystals and acoustic material," Mater. Today 12(12), 34–42 (2009).

[2]Y. Pennec, B. Djafari-Rouhani, J. Vasseur, H. Larabi, A. Khelif, A. Choujaa, S. Benchabane, and V. Laude, "Acoustic channel drop tunneling in a phononic crystal," Appl. Phys. Lett. 87(26), 261912 (2005).

[3]C. Xu, F. Cai, S. Xie, F. Li, R. Sun, X. Fu, R. Xiong, Y. Zhang, H. Zheng, and J. Li, "Phononic crystal tunable via ferroelectric phase transition," Phys. Rev. Appl. 4(3), 034009 (2015).

[4]Y. Wang, Y. Wang, and C. Zhang, "Two-dimensional locally resonant elastic metamaterials with chiral comb-like interlayers: Bandgap and simultaneously double negative properties," J. Acoust. Soc. Am. 139(6), 3311–3319 (2016).

[5]J. Pierre, O. Boyko, L. Belliard, J. Vasseur, and B. Bonello, "Negative refraction of zero order flexural Lamb waves through a two-dimensional phononic crystal," Appl. Phys. Lett. 97(12), 121919 (2010).

[6]Z. Liu, X. Zhang, Y. Mao, Y. Zhu, Z. Yang, C. Chan, and P. Sheng, "Locally resonant sonic materials," Science 289(5485), 1734–1736 (2000).

[7]M. S. Kushwaha, P. Halevi, L. Dobrzynski, and B. Djafari-Rouhani, "Acoustic band structure of periodic elastic composites," Phys. Rev. Lett. 71(13), 2022–2025 (1993).

[8]Z. Zhu and Z. Deng, "Identical band gaps in structurally re-entrant honeycombs," J. Acoust. Soc. Am. 140(2), 898–907 (2016).

[9]A. Martin, M. Kadic, R. Schittny, T. Bückmann, and M. Wegener, "Phonon band structures of three-dimensional pentamode metamaterials," Phys. Rev. B 86(15), 155116 (2012).

[10]J. H. Ma, Z. L. Hou, and B. M. Assouar, "Opening a large full phononic band gap in thin elastic plate with resonant units," J. Appl. Phys. 115(9), 093508 (2014).

[11]C. Sugino, S. Leadenham, M. Ruzzene, and A. Ertur, "On the mechanism of bandgap formation in locally resonant finite elastic metamaterials," J. Appl. Phys. 120(13), 134501 (2016).

[12]L. Raghavan and A. S. Phani, "Local resonance bandgaps in periodic media: Theory and experiment," J. Acoust. Soc. Am. 134(3), 1950–1959 (2013).

[13]G. Bonnet and V. Monchiet, "Low frequency locally resonant metamaterials containing composite inclusions," J. Acoust. Soc. Am. 137(6), 3263–3271 (2015).

[14]Y. Xiao, J. Wen, G. Wang, and X. Wen, "Theoretical and experimental study of locally resonant and bragg band gaps in flexural beams carrying periodic arrays of beam-like resonators," J. Vib. Acoust. 135(4), 041006 (2013).

[15]Y. Xiao, J. Wen, D. Yu, and X. Wen, "Flexural wave propagation in beams with periodically attached vibration absorbers: Band-gap behavior and band formation mechanisms," J. Sound. Vib. 332(4), 867–893 (2013).

[16]M. B. Assouar and M. Oudich, "Enlargement of a locally resonant sonic band gap by using double-sides stubbed phononic plates," Appl. Phys. Lett. 100(12), 123506 (2012).

[17]Y. Chen and L. Wang, "Periodic co-continuous acoustic metamaterials with overlapping locally resonant and Bragg band gaps," Appl. Phys. Lett. 105(19), 191907 (2014).

[18]B. Yuan, V. Humphrey, J. Wen, and X. Wen, "On the coupling of resonance and Bragg scattering effects in three-dimensional locally resonant sonic materials," Ultrasonic 53(7), 1332–1343 (2013).

[19]L. D'Alessandro, E. Belloni, R. Ardito, A. Corigliano, and F. Braghin, "Modeling and experimental verification of an ultra-wide bandgap in 3D phononic," Appl. Phys. Lett. 109(22), 221907 (2016).

[20]S. L. Vatanabe, G. H. Paulino, and E. C. N. Silva, "Maximizing phononic band gaps in piezocomposite materials by means of topology optimization," J. Acoust. Soc. Am. 136(2), 494–501 (2014).

[21]P. Wang, L. Lu, and K. Bertoldi, "Topological phononic crystals with one-way elastic edge waves," Phys. Rev. Lett. 115(10), 104302 (2015).

[22]O. Bilal and M. Hussein, "Ultrawide phononic band gap for combined in-plane and out-of-plane waves," Phys. Rev. E 84(6), 065701 (2011).

[23]V. V. Krylov and F. J. B. S. Tilman, "Acoustic 'black holes' for flexural waves as effective vibration dampers," J. Sound. Vib. 274(3), 605–619 (2004).

[24]V. V. Krylov, "New type of vibration dampers utilizing the effect of acoustic black holes," Acta Acust. Acust. 90(5), 830–837 (2004).

[25]L. Tang, L. Cheng, H. Ji, and J. Qiu, "Characterization of acoustic black hole effect using a one-dimensional fully-coupled and wavelet-decomposed semi-analytical model," J. Sound Vib. 374, 172–184 (2016).

[26]S. Yan, A. Lomonosov, and Z. Shen, "Numerical and experimental study of lamb wave propagation in two-dimensional acoustic black hole," J. Appl. Phys. 119(21), 214902 (2016).

[27]H. F. Zhu and F. Semperlotti, "Phononic thin plates with embedded acoustic black holes," Phys. Rev. B 91(10), 104304 (2015).

[28]H. F. Zhu and F. Semperlotti, "Anomalous refraction of acoustic guided waves in solids with geometrically tapered metasurfaces," Phys. Rev. Lett. 117(3), 034302 (2016).

[29]L. Tang and L. Cheng, "Broadband local resonant bandgaps in periodic structures with embedded acoustic black holes," J. Appl. Phys. 121, 194901 (2017).

[30]E. P. Bowyer and V. V. Krylov, "Experimental investigation of damping flexural vibrations in glass fibre composite plates containing one- and two-dimensional acoustic black holes," Compos. Struct. 107, 406–415 (2014).

[31]T. Zhou, L. Tang, H. Ji, J. Qiu, and L. Cheng, "Dynamic and static properties of double-layered compound acoustic black hole structures," Int. J. Appl. Mech. 9, 1750074 (2017).

[32]L. Tang and L. Cheng, "Enhanced acoustic black hole effect in beams with a modified thickness profile and extended platform," J. Sound. Vib. 391, 116–126 (2017).

[33]P. A. Feurtado, S. C. Conlon, and F. Semperlotti, "A normalized wave number variation parameter for acoustic black hole design," J. Acoust. Soc. Am. 136(2), EL148–EL152 (2014).